THE SYNTHESIS AND CHARACTERIZATION OF MANGANESE FERRITE NANOPARTICLES BASED ON NATURAL IRON ORES

LUFSYI MAHMUDIN*, M. SYAHRUL ULUM, ALBINA LAURENSIA MANALU, SILVANA DWI SUSANTI, RAFIQA WULANDANI

Department of Physic, Faculty of Mathematics and Natural Sciences, Tadulako University, Jl. Soekarno-Hatta Km 9, Kampus Bumi Tadulako Tondo, Palu, Indonesia
*Corresponding Author: lufsym@gmail.com

Abstract

Natural iron ores are abundantly found in Indonesia. Manganese ferrite nanoparticles based on natural iron ores using the coprecipitation method were successfully synthesized with various chloride acid solvent concentrations of 30%, 34%, 37% and ammonium hydroxide precipitator 5 M, 8 M, 10 M. The samples were then dried and characterized which included elemental composition analysis (X-Ray Fluorescence), wave absorption analysis (Ultraviolet-Visible), crystal size and structure analysis (X-Ray Diffraction), and morphology analysis (Transmission Electron Microscopy and Scanning Electron Microscopy). The results of X-Ray Fluorescence analysis show that the iron products from Central Sulawesi's iron ores contain Fe elements of 92.48%. Scanning Electron Microscopy and Transmission Electron Microscopy results show that the manganese ferrite nanoparticle sample experiences agglomeration (clumping). From the X-Ray Diffraction and Ultraviolet-Visible test results, it was found that the size of the nanoparticles ranged from 14.94 -3.21 nm with a cubic crystal structure and absorbed wavelength in 332-337 nm.

Keywords: Coprecipitation, Iron ores, Manganese ferrite, Precipitator.

1. Introduction

In recent times, there has been swift progress in the research related to nanotechnology and nanoparticles (NPs). The NPs which are nano meter scale molecules sized at composed by organic or inorganic materials, possess distinctive properties determined by their size. These unique traits contribute to novel or enhanced capabilities in contrast to larger materials, driving the creation of innovative applications. The preparation of NPs encompasses a diverse range of materials, including metal NPs, metal oxide NPs, non-metal oxide NPs, carbon NPs, and semiconductor NPs [1, 2]. Nanoferrites is a significant type of magnetic metal oxide NPs, distinguished by its unique physical and chemical properties [3, 4]. Ferrite is a ceramic material primarily composed of large proportions of iron oxide mixed with metallic elements [4]. Ferrites are ferrimagnetic materials, where metal as the cation and oxygen as the anion is positioning themselves in the crystal lattice to create various geometric configurations [5]. The chemical formula for ferrite is MFe_2O_4, where M represents cations like Mn^{2+}, Co^{2+}, Ni^{2+}, Cu^{2+}, Zn^{2+}, or others. Ferrite finds extensive use in various technology applications, including magnetic memory devices [6, 7].

Studies conducted in Indonesia have explored the presence of iron ores and analysed its mineral composition. These investigations aim to predict the types of mineral compounds present. Multiple studies have indicated that iron ores in Indonesia holds the potential for the production of Nanoferrites [8-10]. This process is crucial as it provides a solution to harness the abundant iron ores resources in Indonesia. Additionally, it facilitates further research into developing synthesis methods for Nanoferrites using iron sand. These methods are not only cost-effective but also more efficient compared to using commercial chemical precursors [11].

Over recent decades, studies on manganese ferrite ($MnFe_2O_4$) minerals, both in micro- and nano-sizes, have continued to grow due to their properties with soft-magnetic characteristics, including moderate saturation magnetization, high magnetic permeability, and low coercivity [12, 13]. Hence, the $MnFe_2O_4$ NPs material have generated significant interest especially in electronic systems. These NPs also exhibit superparamagnetic behaviour, easy preparation, high crystal symmetry, high electrical resistivity, and excellent chemical stability, which further enhance their appeal [13-15]. In comparison with other ferrite materials such as magnetite, hematite, nickel ferrite, and cobalt ferrite, $MnFe_2O_4$ NPs exhibit a higher biocompatibility, thus, $MnFe_2O_4$ NPs are considered to become one efficient candidate in the biomedical field for various applications, among them magnetic resonance imaging (MRI) and mostly in drug delivery [15-18].

The properties of $MnFe_2O_4$ can be adjusted based on factors such as composition, morphology, and size. These properties are closely linked to the specific synthesis parameters used in the process [19]. Various techniques have been devised for the production of $MnFe_2O_4$ NPs, among them coprecipitation [10, 20], solvothermal [21, 22], hydrothermal [23, 24], and sol-gel [25, 26]. The coprecipitation method was chosen due to its frequent utilization, simplicity, minimal equipment requirements, cost-effectiveness, low-temperature operation (below 100°C), and relatively short processing time [9, 27, 28]. Furthermore, the coprecipitation synthesis method makes producing large quantities of magnetic particles easier than others. This method entangles the simultaneous precipitation

of multiple components present in the solution [29]. Previous studies have explored the synthesis of Nanoferrites using HCl and NH$_4$OH solvents, which led to reduced crystallinity and particle size [30, 31]. The leverage of different solvents on the manganese ferrite structure and the manganese ferrite optical properties from iron ores have not been thoroughly investigated. Understanding these properties and their interrelationships is crucial for comprehending material performance in diverse applications. This paper is focused on MnFe$_2$O$_4$ NPs from natural iron ores in Central Sulawesi as the raw materials. This paper shows some characteristics MnFe$_2$O$_4$ from natural iron ores such as morphology and optical properties based on the varied concentration of HCl and NH$_4$OH under coprecipitation method.

2. Materials and Methods

Manganese ferrite is synthesized from natural iron ores which are originally from Indonesia. In this study, all chemicals and reagents are supporting materials for producing manganese ferrite, and the methods of manganese ferrite production are described in the following section.

2.1. Materials

The iron ore as the raw material was collected from Uekuli village, Tojo Una-Una Regency, Central Sulawesi, Indonesia. Distilled water, ammonium hydroxide, hydrochloride acid, and manganese chloride are the chemicals used in this study and were purchased from Merck (Germany) without further purification.

2.2. The extraction of iron ores

Iron ores, the primary natural material, were crushed to a fine sand-like phase using a geological hammer. Subsequently, it underwent extraction through a permanent magnet, separating magnetite content from impurities. The obtained iron sand was further refined by grinding it in a porcelain mortar. The ground iron ores were sieved through a 180 μm sieve. Any impurities in the magnetite powder (Fe3O4) were removed by washing the sifted powder with distilled water.

2.3. The synthesis of MnFe$_2$O$_4$ NPs using coprecipitation method

In the coprecipitation method, an aqueous precursor solution was prepared by dissolving 8 g Fe3O4 into 25 ml HCl (30%, 34%, 37%) and 4,18 g MnCl2 into 25 ml distilled water and stirred until the solution was homogenous. Furthermore, 60 ml of NH4OH 6,5 M was added into the homogenous solution and magnetically stirred at 60°C for 2 hours. The solution was then placed on top of a magnet until a precipitate was obtained, which was repeatedly washed with distilled water several times and dried at 50°C, as shown in Fig. 1(a). Conversely, the synthesis of MnFe$_2$O$_4$ follows a similar process, with the exception of adding NH4OH at different concentrations (5 M, 8 M, 10 M) into the solution, as illustrated in Fig. 1(b).

2.4. Characterization of Fe$_3$O$_4$ powder and MnFe$_2$O$_4$ NPs

Determination of the elemental composition and the percentage of magnetic components in iron ores of Fe3O4 powder was carried out using X-Ray Fluorescence (XRF) (Shimadzu, EDX-720). X-ray diffraction (XRD) (Shimadzu, XRD-7000L) by radiating Cu-kα radiation (λ = 1.5406 Å) was used to analyse the

phase and crystal structure of $MnFe_2O_4$ NPs. The morphologies and particle sizes of the material were observed and measured using TEM (JEOL, JEM-1400) with selected-area electron diffraction (SAED) measurements. Scanning electron microscope (SEM) (JEOL, JCM-6000PLUS) which is equipped with an energy dispersive X-ray (EDX) spectrometer was used to analyse the elemental compositions, elemental distributions, and the microstructure of the material. The sample absorbance was obtained by analysing the sample using UV-Visible spectroscopy (Shimadzu, UV-1900).
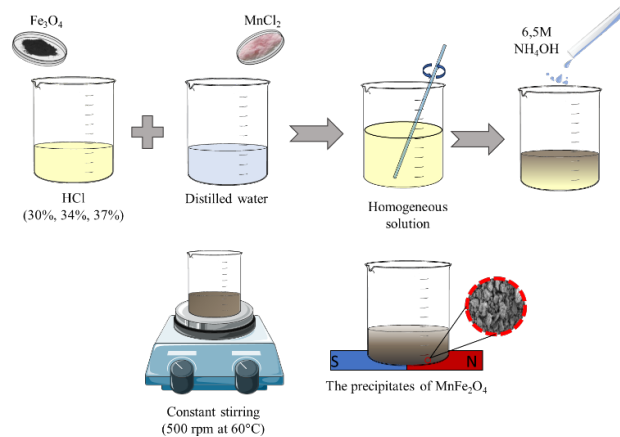
(a) With variations of HCl.
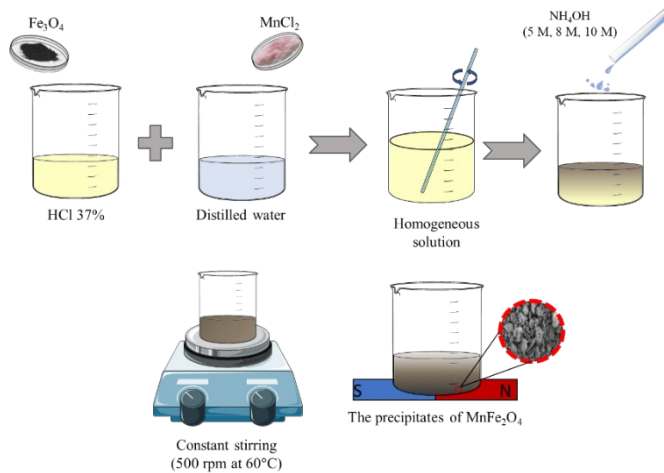
(b) With variations of NH₄OH.

Fig. 1. The schematic synthesis procedure of MnFe₂O₄.

3. Results and Discussion

This section outlined the percentage of iron in the natural iron ores following other elemental compositions. Furthermore, the characteristics of manganese ferrite including optical properties, structure, and morphology are also exposed in detail.

3.1. Iron ores extraction and its composition

The raw material, iron ores, was characterized by the XRF test as shown in Fig. 2. that sample has 6 types of compounds with the dominant content being iron (Fe), manganese (Mn), chromium (Cr), nickel (Ni), titanium (Ti), and other compounds. The percentage obtained is a relative calculation of the total peaks that appear in the absorption pattern, meaning that the area of a particular peak is compared to the overall peak area that appears. Therefore, the resulting data shown in Fig. 2 is the mole`s number for each element content in the iron ores sample.
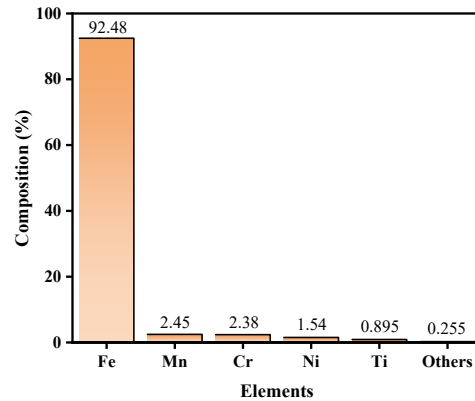

Fig. 2. The composition of iron ores from Central Sulawesi.

3.2. Optical absorption spectra analysis

UV-Vis Spectra shown in Fig. 3 is optical absorption spectra of $MnFe_2O_4$ in liquid cuvette configuration at room temperature at a wavelength range of 200 to 700 nm. The absorption peak of $MnFe_2O_4$ nanoparticles was observed at a wavelength of 336 nm with a strong absorption peak and the region of the peak is in the UV region. Both, the characteristic for sample with HCl variations and NH4OH variations had absorption peak at 332-337 nm.
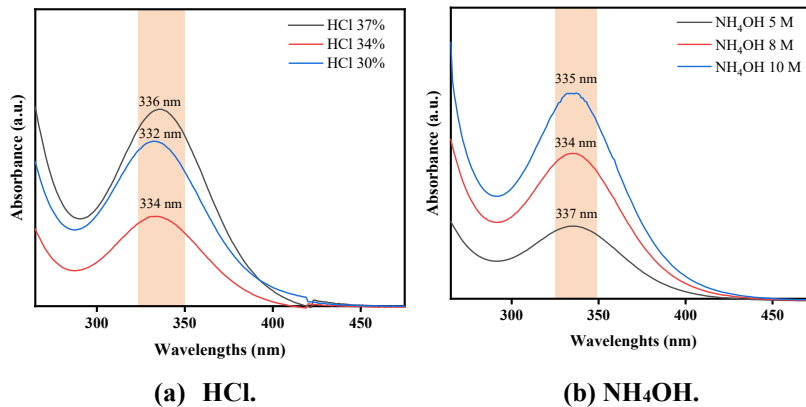

(a) HCl. **(b) NH₄OH.**

Fig. 3. UV-Visible absorbance of $MnFe_2O_4$ with variations.

The results of the UV-Vis spectroscopic analysis can provide details of the size, quantity, and distribution of the nanoparticles formed. There are two possible causes of the wavelength position shift that are related to the size of the nanoparticles. Aggregates are the primary cause, and the ongoing growth of the nanoparticles is the secondary cause. The number of nanoparticles produced is indicated by the absorption value obtained from the UV-Vis spectral photometer reading. In terms of quality, it can be said that the greater the absorption value, the more nanoparticles are produced or the higher the concentration of nanoparticles in the solution.

3.3. Structural and morphological analysis

The purity and crystallinity of $MnFe_2O_4$ were characterized by powder XRD, which are shown in Fig. 4. The sample clearly show the Bragg reflection peaks of $MnFe_2O_4$ related to at 2θ = 30.33, 35.72, 43.34, 53.59, 57.52, 62.94, and 75.23°, which are indexed to the spinel structure of $MnFe_2O_4$ confirmed with JCPDS (Card No: 74-2403) and correspond to the *hkl* plane of (220), (311), (400), (422), (511), (404), and (622) crystal planes, respectively. The XRD data reveals the presence of impurity peaks due to the lack of frequency washing of the sample powder after it is synthesized. The high-intensity peak obtained from the XRD data spectra is further used to determine the average crystallite size of the $MnFe_2O_4$ nanoparticles using Debye Scherrer's formula as shown in equation 1:

$$D = \frac{k\lambda}{\beta \cos \theta} \tag{1}$$

The determination of the average crystallite size of the material was carried out by selecting the highest intensity peak shown in Fig. 4 which is 311 and substituting the value into equation, Debye Scherrer's formula.
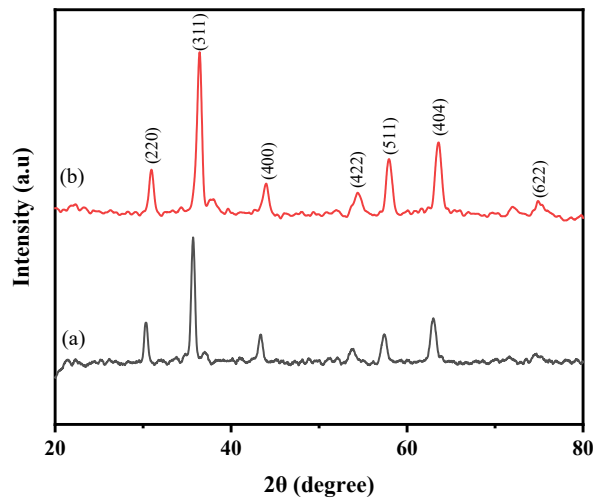

**Fig. 4. XRD patterns of MnFe₂O₄ of (a) HCl 37%,
NH₄OH 6,5 M and (b) HCl 37%, NH₄OH 10 M.**

The average crystallite size obtained from Debye Scherrer`s formula is 13-53 nm, confirming nanoscale ferrites. The details of the crystallite size are briefly summarized in Table 1.

The TEM image of synthesized $MnFe_2O_4$ nanoparticles and the corresponding SAED pattern are shown in Fig. 5(a). The observed particle rings on SAED image agree with the XRD value. The d-spacing provided by the SAED pattern was consistent with the d-spacing provided by XRD which corresponds to the *hkl* plane of (220), (311), (400), (422), (511), (404), and (622) crystal planes. The particle size distribution for the sample ranged from 3-30 nm which confirms nanoscale ferrites as seen in Fig. 5(b).

Table 1. Crystallite size of $MnFe_2O_4$.

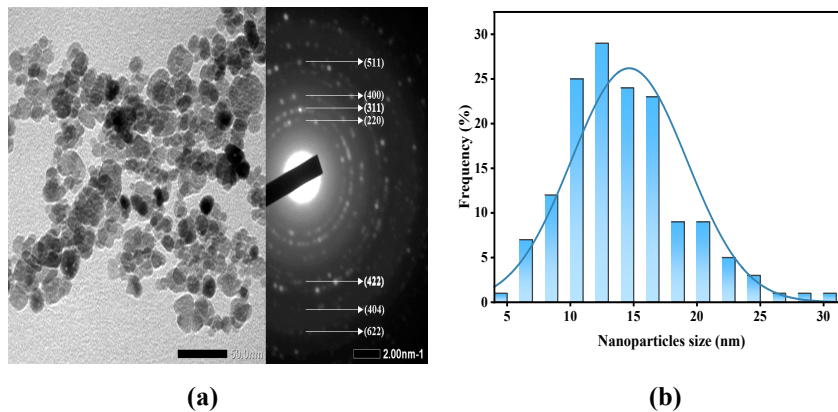| $2\theta(°)$	*hkl*	Size (nm)
30,33	220	53,21
35,72	311	26,98
43,34	400	27,63
53,59	422	14,94
57,52	511	16,48
62,94	404	19,83
75,23	622	28,23

(a)   (b)

**Fig. 5. (a) TEM and SAED pattern of
$MnFe_2O_4$, and (b) distribution size of $MnFe_2O_4$.**

The surface shape of $MnFe_2O_4$ can be evaluated using SEM images. The SEM test results for sample can be seen in Fig. 6. The surface morphology of the sample magnified at 1.000 times magnification has a morphology with a random distribution of particles from the smallest particle size to the largest particle size. The sample test results also showed the presence of irregular fine powder particles, as well as clumping or agglomeration in the sample, this was indicated by the presence of black lumps in the sample.

SEM images show that the manganese ferrite particles produced vary in shape and size, some are small and large on a submicron scale, as evidenced by the SEM images. More small particles are formed than large particles and there are some particles that appear to clump. The morphology image of the particle obtained from SEM analysis shows that the particles are irregular in size so that the shape of the particles is not polydisperse.
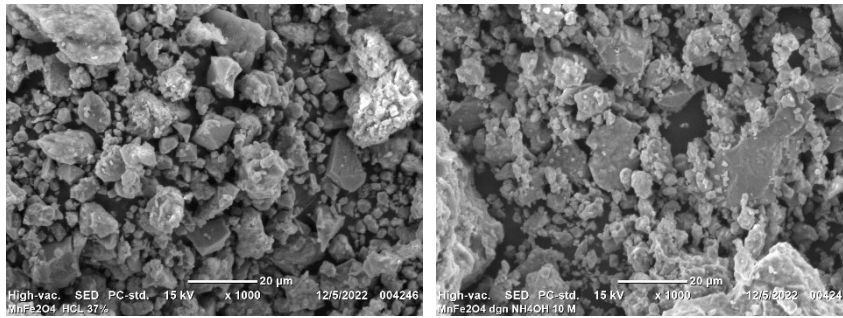
(a) **HCl 37%, NH₄OH 6,5 M.**   (b) **HCl 37%, NH₄OH 10 M.**

Fig. 6. SEM images of MnFe₂O₄.

4. Conclusions

Based on the results and discussion as well as the objectives of this research, it was concluded that $MnFe_2O_4$ NPs had been successfully synthesized from iron ores in Central Sulawesi using the coprecipitation method.

- The crystal structure of the $MnFe_2O_4$ NPs obtained was cubic in shape and the morphology obtained showed that agglomeration occurred in the sample

- The variations in HCl concentration on the optical properties of $MnFe_2O_4$ NPs affect the absorbance value absorbed by the sample. The maximum absorbance value of the manganese ferrite nanoparticle sample was obtained at the highest concentration of HCl

- The higher the concentration of the NH_4OH solution, the higher the absorbance value obtained in optical properties.

Nomenclatures

$Å$	Unit length
D	Body diameter, m
k	Scherrer constant (0.9-1)

Greek Symbols

β	Full width at half maximum of the diffraction peak
λ	Wavelength of $Cu\text{-}K_\alpha$
θ	Diffraction angle

Abbreviations

EDX	Energy Dispersive X-Ray
NPs	Nanoparticles
SAED	Selected Area Electron Diffraction
SEM	Scanning Electron Microscopy
TEM	Transmission Electron Microscopy
XRF	X-ray Fluorescence
XRD	X-ray Diffraction

References

1. Akhlaghi, N.; Najafpour-Darzi, G.; and Younesi, H. (2020). Facile and green synthesis of cobalt oxide nanoparticles using ethanolic extract of Trigonella foenumgraceum (Fenugreek) leaves. *Advanced Powder Technology*, 31(8), 3562-3569.

2. Zhang, Q. et al. (2019). In situ fabrication of Na3V2(PO4)3 quantum dots in hard carbon nanosheets by using lignocelluloses for sodium ion batteries. *Journal of Material Science and Technology*, 35(10), 2396-2403.

3. Akhlaghi, N.; and Najafpour-Darzi, G. (2021). Manganese ferrite ($MnFe_2O_4$) Nanoparticles: From synthesis to application-A review. *Journal of Industrial and Engineering Chemistry*, 103, 292-304.

4. Thakur, P. et al. (2020). A review on MnZn ferrites: Synthesis, characterization and applications. *Ceramics International*, 46(10), 15740-15763.

5. Narang, S.B.; and Pubby, K. (2021). Nickel spinel ferrites: A Review. *Journal of Magnetism and Magnetic Materials*, 519, 167163.

6. Setiadi, E.A. et al. (2018). The effect of synthesis temperature on physical and magnetic properties of manganese ferrite ($MnFe_2O_4$) based on natural iron sand. *Proceedings of the 2nd International Conference on Science (ICOS), Journal of Physics: Conference Series*, Makassar, Indonesia, 12064.

7. Jadhav, V.V.; Mane, R.S.; and Shinde, P.V. (2020). *Bismuth-Ferrite-Based Electrochemical Supercapacitors*. New York, Springer.

8. Togibasa, O.; Akbar, M.; Pratama, A.; and Bijaksana, S. (2019). Distribution of magnetic susceptibility of natural iron sand in the sarmi coast area. *Proceedings of 7th Asian Physics Symposium, Journal of Physics: Conference Series*, Bandung, Indonesia, 1204(1), 12074.

9. Husain, S. et al. (2019). Synthesis and characterization of Fe_3O_4 magnetic nanoparticles from iron ore. *Proceedings of International Seminar on Science and Technology, Journal of Physics: Conference Series*, Palu, Central Sulawesi, Indonesia, 1242(1), 12021.

10. Nengsih, S. et al. (2023). Magnetization study of iron sand from Sabang, Indonesia: The potential of magnetic materials in the photocatalytic field. *Bulletin of Chemical Reaction Engineering and Catalysis*, 18(2), 344-352.

11. Yuliantika, D. et al. (2019). Exploring structural properties of cobalt ferrite nanoparticles from natural sand. *Proceedings of International Conference on Condensed Matters and Advanced Materials (IC2MAM 2018), IOP Conference Series: Materials Science and Engineering*, Jawa Timur, Indonesia, 515, 12047.

12. Liu, C.; Zou, B.; Rondinone, A.J.; and Zhang, Z.J. (2000). Reverse micelle synthesis and characterization of superparamagnetic $MnFe_2O_4$ spinel ferrite nanocrystallites. *The Journal of Physical Chemistry B*, 104(6), 1141-1145.

13. Vamvakidis, K. et al. (2014). Reducing the inversion degree of $MnFe_2O_4$ nanoparticles through synthesis to enhance magnetization: Evaluation of their 1 H NMR relaxation and heating efficiency. *Dalton Transactions*, 43(33), 12754-12765.

14. Mary Jacintha, A.; Umapathy, V.; Neeraja, P.; and Rex Jeya Rajkumar, S. (2017). Synthesis and comparative studies of $MnFe_2O_4$ nanoparticles with

different natural polymers by sol–gel method: Structural, morphological, optical, magnetic, catalytic and biological activities. *Journal of Nanostructure in Chemistry*, 7, 375-387.

15. Asghar, K.; Qasim, M.; and Das, D. (2020). Preparation and characterization of mesoporous magnetic $MnFe_2O_4$ $mSiO_2$ nanocomposite for drug delivery application. *Materials Today: Proceedings*, 26, 87-93.

16. Tromsdorf, U.I. et al. (2007). Size and surface effects on the MRI relaxivity of manganese ferrite nanoparticle contrast agents, *Nano Letter*, 7(8), 2422-2427.

17. Baig, M.M. et al. (2019). Optimization of different wet chemical routes and phase evolution studies of $MnFe_2O_4$ nanoparticles, *Ceramics International*, 45(10), 12682-12690.

18. Peters, J.A. (2020). Relaxivity of manganese ferrite nanoparticles. *Progress in Nuclear Magnetic Resonance Spectroscopy*, 120-121, 72-94.

19. Zeng, H.; Rice, P.M.; Wang, S.X.; and Sun, S. (2004). Shape-controlled synthesis and shape-induced texture of $MnFe_2O_4$ nanoparticles. *Journal of the American Chemical Society*, 126(37), 11458-11459.

20. Anggraini, V.; Putra, R.A.; and Fadlly, T.A. (2021). Synthesis and characterization of manganese ferrite ($MnFe_2O_4$) nanoparticles by coprecipitation method at low temperatures, *Proceedings of the 2nd International Conference on Science, Technology, and Modern Society (ICSTMS 2000), Advances in Social Science, Education and Humanities Research*, 576, 118-122.

21. He, F.; Ji, Y.; Wang, Y.; and Zhang, Y. (2017). Preparation of bifunctional hollow mesoporous $Fe0@C@MnFe_2O_4$ as Fenton-like catalyst for degradation of Tetrabromobisphenol A. *Journal of The Taiwan Institute of Chemical Engineers*, 80, 553-562.

22. Liu, Z.; Chen, G.; Li, X.; and Lu, X. (2021). Removal of rare earth elements by $MnFe_2O_4$ based mesoporous adsorbents: Synthesis, isotherms, kinetics, thermodynamics. *Journal of Alloys and Compounds*, 856, 158185.

23. Kwon, J. et al. (2017). Facile hydrothermal synthesis of cubic spinel AB_2O_4 type $MnFe_2O_4$ nanocrystallites and their electrochemical performance. *Applied Surface Science*, 413, 83-91.

24. Chen, G. et al. (2019). Novel magnetic $MnO_2/MnFe_2O_4$ nanocomposite as a heterogeneous catalyst for activation of peroxymonosulfate (PMS) toward oxidation of organic pollutants. *Separation and Purification Technology*, 213, 456-464.

25. Wang, G. et al. (2018). Removal of norfloxacin by surface Fenton system ($MnFe_2O_4/H_2O_2$): Kinetics, mechanism and degradation pathway. *Chemical Engineering Journal*, 351, 747-755.

26. Asiabar, B.M.; Karimi, M.A.; Tavallali, H.; and Rahimi-Nasrabadi, M. (2021). Application of $MnFe_2O_4$ and AuNPs modified CPE as a sensitive flunitrazepam electrochemical sensor. *Microchemical Journal*, 161, 105745.

27. Wu, S. et al. (2011). Fe_3O_4 magnetic nanoparticles synthesis from tailings by ultrasonic chemical co-precipitation. *Materials Letters*, 65(12), 1882-1884.

28. Setiadi, E.A. et al. (2016). The synthesization of Fe_3O_4 magnetic nanoparticles based on natural iron sand by co-precipitation method for the used of the adsorption of Cu and Pb ions. *Proceedings of 8th International Conference on*

Physics and its Application (*ICOPIA*), *Journal of Physics: Conference Series*, Denpasar, Indonesia, 776, 12020.

29. Laurent, S. et al. (2008). Magnetic iron oxide nanoparticles: Synthesis, stabilization, vectorization, physicochemical characterizations, and biological applications. *Chemical Reviews*, 108(6), 2064-2110.

30. Rahmi; Faturrahmi; Lelifajri; and PurnamaWati, F. (2019). Preparation of magnetic chitosan using local iron sand for mercury removal. *Heliyon*, 5(5), e01731.

31. Rianna, M. et al. (2019). The effect of Mg-Al additive composition on microstructure, magnetic properties, and microwave absorption on $BaFe_{12-2x}Mg_xAl_xO_{19}$ (x= 0–0.5) material synthesized from natural iron sand. *Materials Letters*, 256, 126612.